

Spark-Plasma Sintering (SPS) of various conventional and nanostructured powders

Ciofu Florin, Nioata Alin

SC ROMINEX SA Timisoara-filiala Tg-Jiu, Universitatea "Constantin Brâncusi"-Tg-Jiu

Keywords: plasma, powders, sintering, crystal-growth.

Abstract: Aim of this study is the evaluation of the spark-plasma-sintering method and its suitability for the compaction of various ceramic and metallic, conventional and nanostructured powders (titanium oxide, titanium carbonitride, copper). It should be demonstrated if this new compaction method is qualified to combine a high sintering density with an inhibited grain-growth. The compacted samples were investigated by Xray diffraction, Scanning-Electron-Microscopy, Transmission-Electron-Microscopy and metallographic methods. The results were compared with the data obtained with conventional sintering procedures.

1.Introduction.

The problem of obtaining fully dense nanostructured bulk samples is of essential significance in various fields of materials engineering due to their peculiar mechanical, electrical, optical, and magnetic properties. Aim of this study is the investigation of the sintering process of conventional and nanostructured powder samples by means of the spark-plasma-sintering method and to compare the results with conventional sintering techniques.

Several materials were selected for this study concerning their different electric conductivity and their diverse melting temperatures. Titanium oxide as a non-conductive ceramic material, titanium carbonitride as a non-oxidic, conductive material with high melting temperature and copper as a metallic phase with low melting point were taken under consideration. Here the possible applications of this technological interesting materials will not be discussed further.

The spark-plasma-sintering method can be roughly compared with the conventional hot press. Additionally a pulsed electric current is applied directly to the graphite mold. The SPS method comprises three main mechanisms of action: a) the application of uniaxial pressure, b) the application of pulsed voltage, and c) the resistance heating of graphite dies and sample. Nevertheless, an exact interpretation of the microscopic effect of the SPS has not been achieved. It is obvious that the efficiency of this method is influenced by electric and thermal properties of the sample.

2.Experimental procedure.

Two different titanium oxide powders were used: 1) Nanophase Technologies Corp. NanoTek titanium dioxide powder (lot number T81117-01), containing anatase, only minor amounts of rutile, average particle size 40 nm and a specific surface area of 38 m²/g according to data from the supplier; 2) Kerr-McGee Pigments (Germany) Tronox TR110 (lot number 0027C17) an anatase powder with an average particle size of 0,20µm.

The powder sample Titanium Carbonitride Nanopowder Lot 2002/1, from Plasma Ceramics Technologies Inc., Latvia, was used for the compaction experiments also. this powder was synthesized by ultra-rapid condensation from the gas phase (high frequency

plasma). Following composition was determined by chemical analysis: N7,7%; C12,7%;O2,7%.

Two copper powder samples were used: 1) Copper MP45 from Norddeutsche Affinerie AG Germany, and 2) Nanocopper powder from Argonide Corporation, FL, USA.

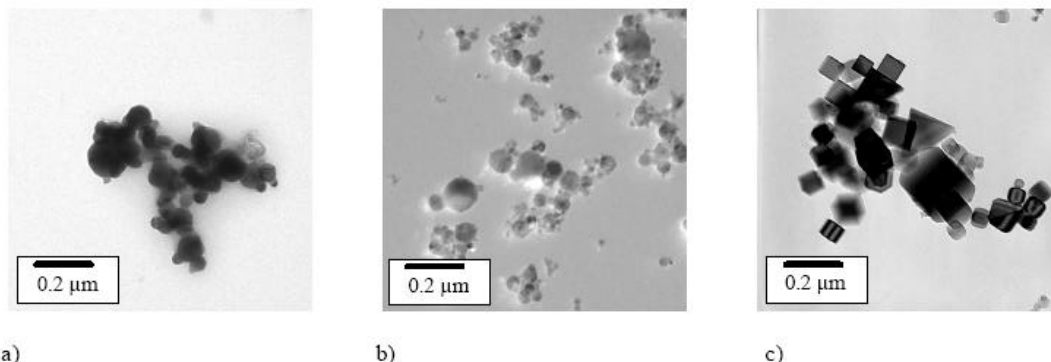


Figure 1: TEM micrographs of the investigated nanostructured powder before compaction: a) copper, b) titanium oxide, c) titanium carbonitride; field of view approximately 1 μ m.

An amount of several grams of the noncompacted titanium oxide and titanium carbonitride powders were loaded without any pressure aids in a graphite die (15 mm diameter) and punch unit. Already precompacted copper tablets were inserted in the graphite die. These tablets were prepared by means of conventional uniaxial pressing-avoiding an extensive contact with the atmosphere.

A low internal pressure (several Pa, air) was applied at the beginning of the sintering experiment. During the sintering process the pressure increases to 300Pa while reaching maximal temperature. The pressure applied at the punch unit reached a maximum of 7 to 15 MPa. The used electric current was typically 500A at 700°C and 800A at 1000°C. The corresponding voltage lay between 3,0V and 4,5V respectively. The electric current was pulsed periodically with 14 pulses/sec (2 of 14 pulses off as a recovery time).

The temperature was measured by means of a pyrometer on the surface of the graphite die cylinder. A temperature gradient between the measured temperature and the sample is expected. The internal pressure was controlled by a Pirani element. All parameters were monitored during the experiment. The heating rate lay at 100°C/min, the dwelling time was 1 min. In figure 2 a schematic of this device is displayed.

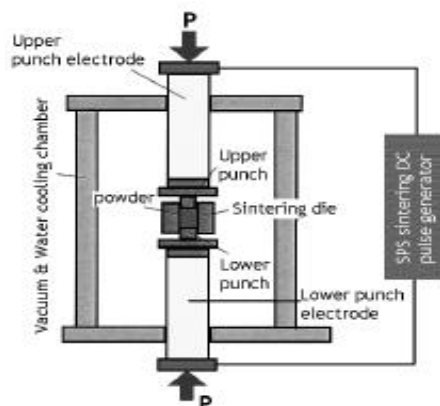


Figure 2: Schematic drawing of the applied SPS apparatus.

3.Characterisation.

The determination of the compacted samples was performed using Archimedes principle, Ethanol was used as a liquid medium. The values for the relative densities were calculated assuming a theoretical density for rutile of $4,26 \text{ g/cm}^3$, titanium carbonitride of $5,1 \text{ g/cm}^3$ and copper of $8,96 \text{ g/cm}^3$. The micrographs of the uncompacted nanopowder were obtained with a transmission electron microscope (TEM) CM 20 (Philips, Netherlands) using an acceleration voltage of 200 kV. The microstructural investigation of the fracture surface of the compacted samples was conducted by using a scanning electron microscope (SEM) DSM-950 (C.Zeiss, Germany). The acceleration voltage was between 5 and 20 kV.

The phase characterisation of the samples and the subsequent crystallite size determination with X-ray powder diffractometry (XRD) were performed using an Philips X'Pert Powder diffractometer with Bragg-Brenantano geometry using copper $\text{K}\alpha_{1,2}$ radiation at 40 kV and 40 mA. The measurements were performed in step-scan mode over the range $5\text{-}85^\circ 2\theta$.

For the determination of d several well defined diffraction peaks with a diffraction angle in the range between $25^\circ 2\theta$ and $60^\circ 2\theta$ were used and an average value for the crystallite size was subsequently calculated using Scherrers's equation. These data are not fully consistent with the observed grain size in the SEM. An increasing crystallite size (XRD) corresponds with an even larger growth of the grain size (SEM). This difference is generated by a possible polycrystalline structure of the rutile grains.

4.Results and discussion.

Titanium oxide. Figure 3 a) shows the obtained densities of conventional and nanostructured TiO_2 samples as a function of the sintering temperature regardless of the dwell time. The lower sintering temperature of the TiO_2 nanopowder in comparison to the conventional samples is obvious. At an equal temperature a higher density can be obtained in the nanostructured samples. This difference occurs during conventional sintering as well as in the SPS experiments. Generally the SPS method generates more dense samples than conventional sintering, although the effective temperatures of both methods are difficult to compare due their different dynamic measurement conditions.

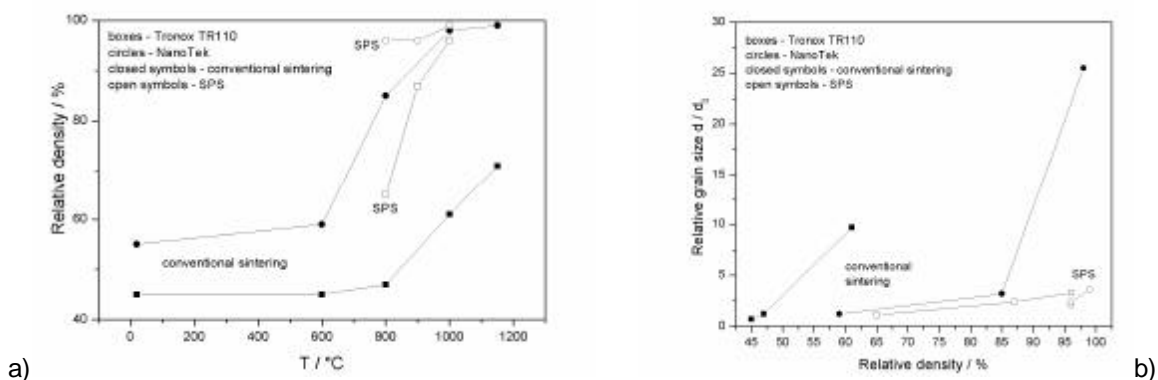


Figure 3: a) relative density as a function of the sintering temperature. The SPS method displays a significant increase of density compared to conventional sintering. b) relative grain size as obtained by WRD, plotted as a function of the relative density. The SPS method shows a significant smaller grain growth.

X-ray powder diffraction measurements were performed of each compacted sample to detect the phase composition and the full width at half maximum of the diffraction maxima (XRD-traces not displayed here). In figure 3 b) the dependency of the grain growth d/d_0 as a function of the relative value of compaction is shown. The values were obtained according to the Scherrer formula, d_0 denotes the crystallite size of the uncompacted powder. In table 1 all data for the sintered samples are shown for SPS experiments and conventional experiments, respectively.

Material	Technique	T (°C)	t (min)	ρ (g/cm ³)	ρ_{rel} (%)	d (nm)	d/d_0
NanoTek	SPS	800	1	4,08	96	78	2,1
NanoTek	SPS	900	1	4,08	96	90	2,4
NanoTek	SPS	1000	1	4,23	99	133	3,6
TronoxTR110	SPS	800	1	2,77	65	146	1,1
TronoxTR110	SPS	900	1	3,69	87	325	2,4
TronoxTR110	SPS	1000	1	4,11	96	441	3,3
NanoTek	conv.	600	120	2,50	59	44	1,2
NanoTek	conv.	800	120	3,63	85	118	3,2
NanoTek	conv.	1000	120	4,17	98	945	25,5
TronoxTR110	conv.	600	120	1,92	45	95	0,7
TronoxTR110	conv.	800	120	1,99	47	159	1,2
TronoxTR110	conv.	1000	120	2,58	61	1315	9,7

Table 1: Several by SPS and by conventional sintering experiments compacted. (T=sintering temperature, t= dwell time at maximal temperature, ρ =density of the compacted sample, ρ_{rel} =corresponding relative density, d=crystallite size obtained by X-ray diffraction, d/d_0 =relative grain growth, technique=corresponding compaction method.)

The grain growth in the conventional sintering experiments is therefore significant higher in comparison to SPS-samples with an equivalent grade of densification. The activation energy of the grain-growth reaction during the spark-plasma sintering process is significant reduced. It is most likely that the activation energy of the grain growth reaction is reduced by spark plasma mechanism.

Titanium carbonitride. It is pretty difficult to obtain dense samples of this melting material. Figure 4 a) shows the relative density obtained by means of various sintering methods as a function of the sintering temperature. Regardless of the difficulty to compare experiments of various sintering times and different temperature measurement circumstances, the SPS process shows high densities at comparatively low temperatures. The conventional sintering process is not capable to produce high densities of this carbonitride sample even with comparatively long dwelling times (120 min).

For the evaluation of the sinter process the dynamics of the grain growth is crucial. In figure 4 b) the relative grain (or crystallite) growth d/d_0 as obtained by XRD is plotted as a function of the relative density for several samples. Here the SPS method can be identified by a more favourable grain growth to density ratio.

In table 2 a compilation of all these compaction data including various parameters of the conventional sintering experiments is given. A significant difference between the various sintering methods can also be determined looking at the fracture surface.

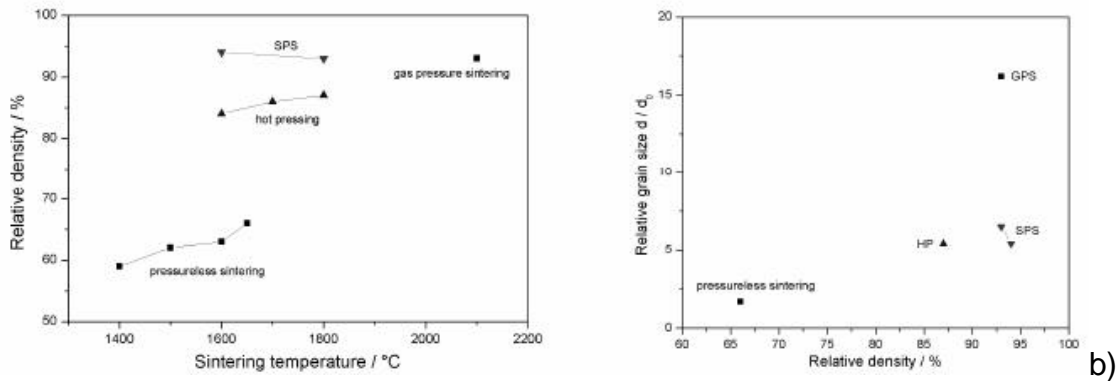


Figure 4: a) relative density of nanostructured titanium carbonitride as a function of the sintering temperature. The various applied sintering methods are indicated. b) relative XRD obtained grain size of titanium carbonitride samples compacted by various indicated methods, plotted as a function of the relative density. The SPS method shows a more favourable grain growth to density ratio.

Material	Technique	T (°C)	t (min)	ρ (g/cm ³)	ρ_{rel} (%)	d (nm)	d/d ₀
PCT 1 Ti(C,N)	SPS	1600	1	4,78	94	205	5,4
PCT 1 Ti(C,N)	SPS	1800	1	4,76	93	246	6,5
PCT 1 Ti(C,N)	GPS	2100	45	4,76	93	616	16,2
PCT 1 Ti(C,N)	HP	1600	60	4,26	84	616	16,2
PCT 1 Ti(C,N)	HP	1700	60	4,38	86	616	16,2
PCT 1 Ti(C,N)	HP	1800	60	4,44	87	205	5,4
PCT 1 Ti(C,N)	conv	1500	120	3,16	62	205	5,4
PCT 1 Ti(C,N)	conv	1600	120	3,22	63	205	5,4
PCT 1 Ti(C,N)	conv	1650	120	3,35	66	64	1,7

Table 2: Several by means of SPS and by various conventional sintering experiments compacted titanium carbonitride sample. (T=sintering temperature, t=dwell time at maximal temperature, ρ =density of the compacted sample, ρ_{rel} =corresponding relative density, d=crystallite size obtained by X-ray diffraction, d/d₀=relative grain growth, technique=corresponding compaction method, SPS=spark plasma sintering, GPS=gas presurre sintering under 8MPa N₂, HP hot pressing 30 MPa uniaxial pressure, conv.=conventional pressureless sintering under N₂)

The SPS compacted samples (SEM micrographs in figures 5 a) and b) show a complete recrystallized texture with grains of various diameters between 0,3 and 5 μm with a relative homogenous distribution around 1 μm . The few larger grains are possibly generated by initial agglomerates in the source powder.

The titanium carbonitride sample was filled in the graphite die before the sinter experiment without any de-agglomeration treatment as ultrasonic conditioning or mixing under liquid phase. On the other hand the GPS compacted sample show a complete different fracture surface (figure 6). Clusters with a grain less than 1 μm size are observed in a matrix with a glassy appearance.

The SPS method is suitable for combing high sintering densities and comparatively low grain-growth of the titanium carbonitride compounds. Further experiments with samples of different grain-size and different carbide to nitride ratio should be performed. The oxygen content and the concentration of the free carbon in the various samples should also be considered.

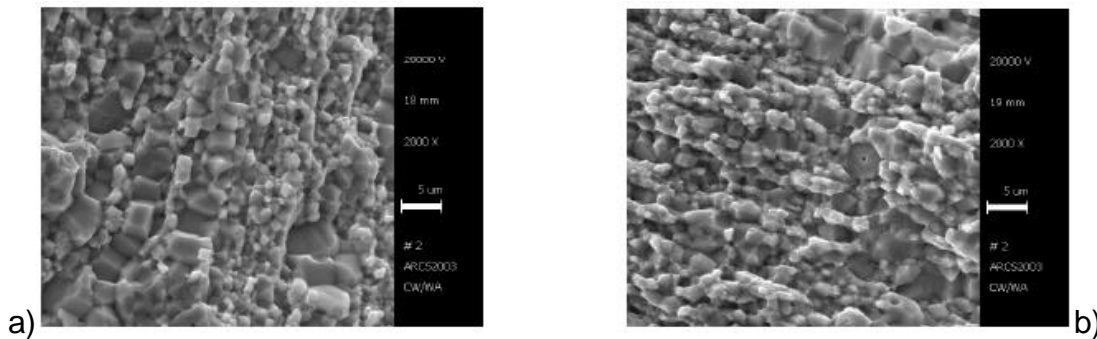


Figure 5: Scanning electron microscope (SEM) micrograph of nanostructured titanium carbonitride powder after compaction by means of SPS at a) 1600°C for 1 min (fracture surface) and b) 1800°C for 1 min (fracture surface).

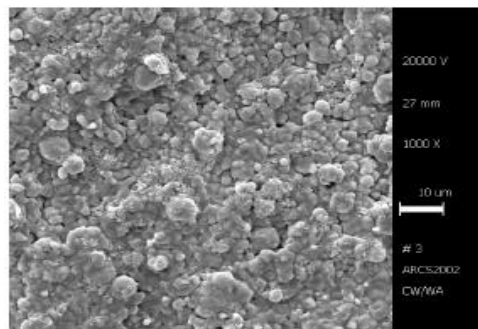


Figure 6: Scanning electron microscope (SEM) micrograph of nanostructured titanium carbonitride powder after compaction by means of GPS at 2100°C for 45 min (fracture surface).

Copper. Two different powder samples were used for the compaction experiments. In each case the preparation of this material is complicated by its oxidation behaviour. During the sintering process the oxygen adsorbed on the surface on the copper particles and the remaining atmospheric oxygen present in the apparatus reacts with the copper forming cuprite, Cu_2O . It should be noted that only 1% oxygen is capable forming almost 10% cuprite after complete reaction. The fraction of cuprite in the Argonide powder is much higher than in the MP45 sample. This could be caused by a finer grain size and a more reactive surface of the Argonide powder.

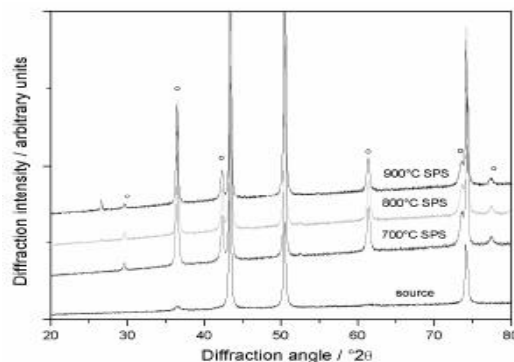


Figure 7: XRD diffractograms between 20° and 80° 2θ for nanostructured copper samples compacted by SPS at 700°C, 800°C, and 900°C and for the corresponding source material. The diffraction maxima belonging to the cuprite phase are indicated with circled.

Figure 7 shows the diffractograms of the Argonide copper powder before compaction, and after SPS-compaction at 700°C, 800°C, and 900°C, respectively. In the source material almost no cuprite is present while during the sintering experiments the intensity of the cuprite reflections is increasing. In figure 8 a micrograph of the polished surface (optical microscopy) after SPS at 700°C and 800°C, respectively is given.

The fine distribution of the cuprite phase (dark grey) in the copper matrix can be seen. Observing a larger area of the sample the homogeneity is not so well defined. The amount of cuprite obtained from calculation from polished surface is 40% at 700°C and 57% after sintering at 800°C, respectively. Further quantitative phase analysis of the diffraction measurements should be undertaken.

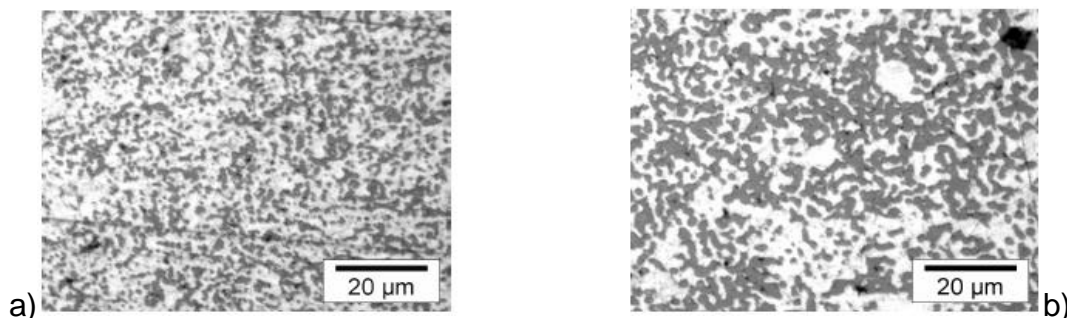


Figure 8: Pictures of the polished cross section (light microscopy) of nanostructured copper after SPS compaction at a) 700°C and b) 800°C.

Calculating relative densities with these composition, (density of cuprite of 6,1 g/cm³) the corresponding densities are 6,46 g/cm³ (82%) and 6,29 g/cm³ (86%). The concentration of cuprite in the MP45 samples does not exceed 5%. The SPS compaction experiments of the copper under air show only a slight advantage compared to the conventional sintering experiments performed under hydrogen atmosphere.

The presence of oxygen should be avoided during possible future experiments. In table 3 a compilation of the compaction data including density and crystallite grain size is given.

Material	Technique	T (°C)	t (min)	? (g/cm ³)	d (nm)	d/d ₀
Cu Argonide	SPS	700	1	6,46	113	2,2
Cu Argonide	SPS	800	1	6,29	121	2,3
Cu Argonide	SPS	900	1	6,45	90	1,7
Cu MP45	SPS	700	1	7,54	103	2,4
Cu MP45	SPS	800	1	7,29	86	2,0
Cu MP45	SPS	900	1	7,32	73	1,7
Cu Argonide	conv	600	120	7,15	275	5,3
Cu Argonide	conv	700	120	6,60	382	7,3
Cu Argonide	conv	800	120	6,82	296	5,7
Cu MP45	conv	600	120	7,93	323	7,5
Cu MP45	conv	700	120	7,65	930	21,6

Table 3: Several by SPS and by conventional sintering experiments compacted copper samples; relative densities are not given due to the uncertainty of the quantitative phase composition. (T=sintering temperature, t=dwell time at maximal temperature, ?=density of the compacted sample, d=crystallite size obtained by X-ray diffraction, d/d₀=relative grain growth, technique=corresponding compaction method.)

A possible application of a similar distribution of cuprite in copper has been described in respect of the thermophysical properties of cuprite as an application for combining a reduced thermal expansion of the copper/cuprite composite with a still reasonable thermal conductivity. The SPS method could be a method to obtain a defined cuprite concentration and grain size by varying the sintering parameters.

5. Bibliography.

- [1] Angerer P., Yu L. G., Khor K. A. – Spark Plasma Sintering (SPS) of nanostructured and conventional Titanium Oxide powders. Mater. Sci. and Eng. A. submitted
- [2] Campbell J., Fahmy Y., Conrad H. – Influence of an electric field on the plastic deformation of fine-grained Al_2O_3 , Metallurgical and materials transactions, 1999
- [3] Fultz B. & Howe J.M. – Transmission Electron Microscopy and Diffractometry of Materials, (Springer-Verlag, Heidelberg).
- [4] Groza, J.R. & Zavaliangos A.– Sintering activation by external electrical field. Mater. Sci. and Eng. A 287, 171-177.
- [5] Groza J.R. – Field activated sintering, ASM Handbook, Volume 7, 1991
- [6] Holm R. – Electric contacts: Theory and application, Springer-Verlag New York Inc.
- [7] Kamiya A. – Observation of sample sintering temperature by the plasma activated sintering (PAS) furnace. J.Mater. Sci. Lett. 17, 49-51.
- [8] Okamoto K., Kondo Y., Abe T., Aono Y – United States Patent Application No 2002/0145195A1.
- [9] Omori M. – Sintering, consolidation, reaction and crystal growth by the spark plasma system (SPS), Materials Science and Engineering, 2000.